The optimum temperature of the superconductor coil is near 10°K; at higher operating temperatures, the current density begins to drop, causing the mass of the magnet and insulation to increase more than the mass of the radiator and power supply decreases; at lower temperatures, the opposite trends occur.

A digital computer program has been used to determine the magnetic field intensity inside the space vehicle. The maximum allowable value probably is of the order of 500 gauss; higher values affect the operation of standard relays and many other devices. Increasing the radius of the coils will reduce the magnetic fields inside the vehicle at some cost in shielding mass. It may be more advantageous to incorporate special shielded regions inside the space ship for housing the sensitive components. It should also be mentioned that future advances in super-conductivity and low-temperature cooling systems will greatly benefit active shields, whereas no avenue for significant improvement in material shields is foreseen.

References

[1] Levy, R. H., "Radiation Shielding of Space Vehicles by Means of Superconducting Coils," *ARS Journal*, Vol. 31, 1961, p. 1568.

[2] Bhattacharjie, A. and Michael, I., "Mass and Magnetic Dipole Shielding Against Electrons of the Artificial Radiation Belt," *AIAA Journal*, Vol. 2, No. 12, Dec. 1964, pp. 2198–2201.

[3] Levine, S. H. and Lepper, R., "Analogue Studies of Magnetic Shields," *AIAA Journal*, Vol. 6, No. 4, April 1968, pp. 695–701.

[4] Levine, S. H. and Lepper, R., "Magnetic Shield Simulator," *Annual Technical Proceedings*, Institute Environmental Sciences, 1965.

[5] Levine, S. H., Bhattacharjie, A., and Lepper, R., "Forbidden Regions Produced by Two Parallel Dipoles," *AIAA Journal*, Vol. 4, No. 4, April 1966, p. 654–658.

[6] Stormer, C., Chapter II, *The Polar Aurora*, Oxford University Press, New York, 1955, p. 229.

[7] Vette, J. I., "Models of the Trapped Radiation Environment," Vol. I, *Inner Zone Protons and Electrons*, and Vol. II, *Inner and Outer Zone Electrons*, NASA SP-3024, 1966.

[8] Fortney, R. E. and Duckworth, G. D., "The Importance of Radiation Anisotropy in Dose Calculations," *Second Symposium on Protection Against Radiation in Space*, NASA SP-71,1964.

[9] Levine, S. H. and Lepper, R., "Analogue Studies of Active Radiation Shielding," AFFDL-TR-67-66, June 1967, Air Force Flight Dynamics Lab.

[10] Janossy, L., Chapter VII, *Cosmic Rays*, Oxford at the Clarendon Press, 1950, p. 270.

[11] Montgomery, D. J. X., *Cosmic Ray Physics*, Princeton University Press, Princeton, N.J., 1949, p. 316.

[12] Betterton, J. O. et al., *Superconductors*, Interscience, New York, 1962.

[13] Foner, S., Private Communication, National Magnet Lab., MIT, May 1968.

[14] Little, A. D., "Exploratory Development of a 3.6°K Rotary Stroking Refrigerator," RTDPRNR. 20534, April 14, 1966.

JULY 1971 J. SPACECRAFT VOL. 8, NO. 7

Accelerometer Calibration in the Low-g Range by Means of Mass Attraction

KONRAD REINEL*

Deutsche Forschungs- und Versuchsanstalt fuer Luft- und Raumfahrt e.V., Oberpfaffenhofen, Germany

Mass attraction is used as an acceleration input to calibrate an accelerometer. The upper limit of the acceleration by a reasonable mass size is 10^{-9} g in orbit and 10^{-7} g in the laboratory. The calibration has been carried out in the laboratory for an electrostatic suspended single-axis accelerometer (MESA) with a variable mass attraction. The tilting of the test pad was avoided by a vertical movement of the attracting mass and always checked by a very sensitive tiltmeter. The mass attraction input to the accelerometer was a sine wave with the amplitude of 23×10^{-9} g. The response of the accelerometer to this acceleration input by mass attraction was obtained by computer data reduction. The results of the experiments agree with the scale factor of the accelerometer for higher acceleration inputs. Application of the mass attraction principle as a calibration method of accelerometers for very low accelerations in orbit is proposed.

Nomenclature

a = acceleration of the proof mass along the input axis
A = accelerometer data
d = distance between center of proof mass m and surface of attracting mass M
g = Earth gravity (981 cm/sec²)
I = measurement number
k = edge of lead cube
K = harmonic number
m = proof mass of the accelerometer
M = attracting mass
N = number of data
r = radius of a sphere
R = distance between two mass points
xyz = coordinate system fixed to center of proof mass with x axis along the input axis of the accelerometer
X,Y,Z = position of the attracting mass in the xyz system
γ = universal gravitational constant (6.67×10^{-8} cm³ g^{-1} sec^{-2})
μg = 10^{-6} g
a_I = acceleration of the proof mass during measurement number I
a_o = amplitude of the sinusoidal acceleration

Presented as Paper 70-1030 at the AIAA Guidance, Control and Flight Mechanics Conference, Santa Barbara, Calif., August 17–19, 1970; submitted September 30, 1970; revision received January 15, 1971. This research was accomplished at the Astrionics Laboratory in the George C. Marshall Space Flight Center while the author held a National Research Council Postdoctoral Resident Research Associateship supported by NASA. Thanks are given to B. Walls and G. B. Doane of the Astrionics Laboratory for assistance and support.

* Division Chief, Inertial Techniques and Attitude Simulation, Institut fuer Dynamik der Flugsysteme. Member AIAA.

A_I = accelerometer data of measurement number I
B_I = tiltmeter data of measurement number I
C_K = Fourier coefficient for harmonic number K
F_x = force of mass attraction along x axis
M_i = mass elements of the attracting body

Introduction

GENERALLY, the single-axis accelerometer, used for inertial navigation, is tilted in the Earth's gravitational field for its calibration between ± 1 g and ± 1 μg, where the acting acceleration is a function of the angle between the sensitive accelerometer axis and the local vertical. The input axis is almost horizontal for low-g calibration, and the accuracy of this method is limited by the measurement of a very small angle. The resolution of the best available theodolite is about 0.1 arcsec with an accuracy of 0.2 arcsec. The angle of 0.2 arcsec limits the calibration accuracy to 1.0 μg. This is sufficient for almost every inertial navigation system. An acceleration error of 1.0 μg in an inertial navigation system would cause a position error of about 65 m after 1 hr.

However, some necessary measurements in space require a calibration of the accelerometer far beyond this 1-μg limit. The Apollo application program for example includes the measurement of the gravity-gradient anomalies of the moon with a satellite.[1] Gravity gradient is a function of mass distribution, and mass concentrations near the surface of the moon will generate a deviation of the measured gravity gradient from the calculated gravity gradient of a reference ellipsoid. The gravity-gradient of the moon in a proposed 55-km orbit is about 2×10^3 Eoetvoes units. The required performance of the experiment is to measure 0.5 Eoetvoes units to determine the magnitude and direction of the lunar gravity gradient anomalies.

One Eoetvoes unit is 10^{-9} sec^{-2} or 1.018×10^{-12} g cm^{-1}. If an accelerometer is used as a gravity-gradient sensor at a 2-m distance from the mass center of the satellite, the required threshold is 10^{-10} g.

Because a range of only 10^{-6} g is in the state of the art, the accelerometer must be switched to this high-sensitive range after the large acceleration of the launch. Therefore the final calibration of the accelerometer has to be made in orbit for its low-g application.

An attempt has been made to calibrate an accelerometer in Earth orbit with a centrifuge.[2] (This calibration was limited to 10^{-6} g.) The apparent acceleration is a function of the distance from the rotation center and of the angular velocity. The angular velocity would be as small as 10^{-3} rad/sec for a 10^{-9}-g acceleration of a mass point at a 2.5-cm distance from the rotation center. It would be very difficult to get such a low constant angular velocity in the satellite.

This paper describes the use of the mass attraction of rigid body for the calibration of an accelerometer in the range below 10^{-9} g in a satellite and below 10^{-7} g in the laboratory. The size of the mass that can be handled is the limiting factor. Calibration in the laboratory with the mass attraction method has been carried out and is described. A proposal is made for the calibration of an accelerometer in a satellite.

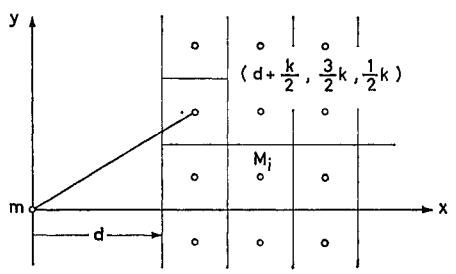

Fig. 1 Attraction of a large body.

Mass Attraction as Calibration Force

For the low-g range, the mass attraction of a smaller rigid body has some advantage over the table tilt calibration method because the acting acceleration is a function of the size of the mass. It is very easy to generate a small acceleration by mass attraction, but there are two problems: The accelerometer must be able to sense this small acceleration, and the system must separate this small input acceleration from much larger background disturbances.

The lower limit of acceleration sensing is given by the threshold of the accelerometer and the requirements for the experiment. The upper limit is given by the size of the mass. Because the mass must change its position to generate a variable additional acceleration input, the mass should be of a size that can be handled. The mass used in the laboratory experiments was about 1000 kg; in a satellite, it might be about 1 kg. Therefore, the corresponding limits of the mass attraction are about 0.05 μg in the laboratory and 0.001 μg in the satellite.

The disturbances in the laboratory are the unknown tilt angle of the accelerometer in the Earth field, tilting of the foundation, bending of the fixture, and changing of the temperature. The disturbances in a satellite are mass attraction of some other parts of the satellite, changing of the temperature, and acceleration by gravity gradient of the orbited planet. Because generally these disturbances cannot be eliminated, they are separated by filtering as discussed in this paper. The input acceleration is changed with a certain frequency, which should not correspond with the frequency of any other acceleration. The input frequency of the mass attraction can be very low. The variation of the mass attraction is either a change in the distance between the accelerometer and the attracting mass or a change in the angle between the sensitive accelerometer axis and the vector of the mass attraction.

Mass Attraction of a Rigid Body

The accelerometer to be calibrated is a single axis device; therefore, only the acceleration component along the input axis is of interest. The proof mass of the accelerometer is m and the large calibrating mass is M. The Cartesian coordinate system xyz has its origin at the center of m and its x axis along the sensitive axis of the accelerometer.

If m and M are two mass points with the positions (0,0,0) and (X,Y,Z), the attraction force F_x in the x direction would be:

$$F_x = \gamma m M X/R^3, \quad R = (X^2 + Y^2 + Z^2)^{1/2} \qquad (1)$$

where γ is the universal gravitational constant in CGS units, and R is the distance between the mass points. The acceleration a of the proof mass along the input axis is

$$a = \gamma M X/R^3 \qquad (2)$$

Equation (2) is also correct if the calibrating mass M is an extended homogeneous sphere. Then R is a sum of the radius of the sphere and the distance d between the center of the proof mass and the surface of the sphere; the radius of the sphere changes with the mass M. The acceleration

Table 1 Acceleration by a lead sphere

Mass, kg	Acceleration, Earth g	Sphere radius, cm
0.15	10^{-10}	1.5
4	10^{-9}	4.4
68	10^{-8}	11.25
4700	10^{-7}	46.3
1.4×10^6	10^{-6}	307
1.4×10^{24}	1	3.07×10^8

of a lead sphere (density of 11.34 g/cm³) along the x axis at a distance of $d = 10.2$ cm from the proof mass is shown in Table 1. For an acceleration of 10^{-7} g the mass would weigh 4700 kg. This is already too much to handle easily in a laboratory. Instead of a sphere an assembly of small cubes was used for the experiments. The mass attraction of a rigid body with an irregular shape is given by a triple integral and has no general analytical solution; but if the distance between the proof mass and the rigid body is large in relation to the size of the body, then the attraction is the same as that of a sphere or a mass point with the same mass.[3] Therefore, the mass M was considered to be cut into small cubes of edge k with an imaginary point mass M_i in the center of each cube (Fig. 1). The mass attraction is computed for every cube and the sum of all cubes is the attraction of the whole body. The error of this approximation is a function of the ratio of the edge k of the cube to the distance R. The cube edge should be always less than a half of the distance for a 10^{-3} accuracy.

In the experiment the distance between the center of the nearest cube and the center of the proof mass was 10.2 cm. The edge of the cube was 5.1 cm. In the computation of the mass attraction, the cylindrical proof mass of the MESA was also considered as a mass point. The error of this approximation is less than 10^{-3} for all cubes.

The attracting mass was limited to less than 1500 kg by the available suspension capability. Therefore, an optimization was made for the arrangement of the cubes. The mass attraction for every possible cube in a space of 20 k × 20 k × 10 k was calculated. The first 900 most attracting cube locations were chosen for the attracting mass of the experiment. The body that was used in the experiments was a compound of 100 lead cubes with 10.2-cm length each and 100 lead cubes with 5.1-cm length each.

The input acceleration could have been varied by changing the distance d between the proof mass and the surface of the attracting body. To get a change in the attraction of 0.07 μg, the mass would have been moved about 76.2 cm along the input axis of the accelerometer. But this movement of the lead mass was not possible in the laboratory.

Calibration in the Laboratory

Experiment Setup

The movement of the lead mass on the floor would cause some additional tilting of the test pad. Therefore, a suspension of the mass on an I-beam of the ceiling was considered best. But in this case, the colinear movement of the mass along the horizontally aligned accelerometer input axis would require too large a force pulling horizontally. The chosen change of the mass attraction along the accelerometer input axis was a movement along the vertical.

The vertical movement changed the acceleration component along the input axis because the angle between the input axis and the mass attraction vector was variated. The lead mass was lowered and raised with an electrical hoist. A drawing of the experimental setup for the calibration of the accelerometer using this mass attraction scheme is shown in Fig. 2. The experimental setup allowed a total vertical travel of just 30.5 cm. To get the maximum change in the

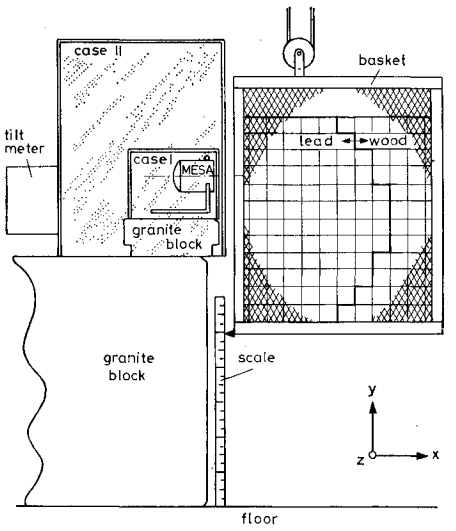

Fig. 2 Test setup for the calibration of the miniature electrostatic accelerometer in the laboratory.

acceleration input the mass is moved vertically between 12.7 cm and 43.2 cm below the zero position.

For the harmonic determination, the input acceleration for as few as four points of a wave length of vertical position were recorded: middle, maximum, middle, minimum. The maximum position was at a vertical distance of 12.7 cm below the zero position, the minimum position was 43.2 cm below, and the middle position was 28.6 cm below. The middle position was chosen so that the input acceleration at that position is the average of those occurring at maximum and minimum positions. The succeeding run through these positions produces a sine-wave input a_I to the accelerometer

$$a_I = a_o \sin(\pi I/2), \qquad a_o = (23.0 \pm 0.2) \times 10^{-9}\, g \quad (3)$$

With a movement larger than 100 cm, the input amplitude a_o could be as high as 0.037 μg with the same mass and the same components.

To demonstrate low-g accelerometer calibration, the Miniature Electrostatic Accelerometer (MESA),[4] manufactured by Bell Aerosystems, was used. The MESA is a single-degree-of-freedom accelerometer with an electrostatically suspended proof mass. This proof mass is a thin-walled beryllium cylinder with a flange for pickoff and restraint. The cylinder length is 2.915 cm and the inner diameter is 1.268 cm. The distance between the center of the float and the mounting surface of the accelerometer is 3.1 cm.

The proof mass suspension force is adjustable to different accelerations of the environment. A pulsed force rebalance technique is used to constrain the proof mass along its sensitive axis. The pulse rate is proportional to the acceleration along the cylinder axis (input axis). The MESA that was used had two ranges: low-g range with 10.21 pps/μg and high-g range with 1.024 pps/μg. For the entire experiment the MESA was used in the low-g range. The technical data

Table 2 Results of the experiments

Experiment	Acceleration input, μg	Accelerometer response 10^{-2} pps	Random noise 10^{-2} pps	Signal response 10^{-2} pps	Standard deviation 10^{-2} pps
1	0.023	27.80	2.17	25.63	5.59
2	0.023	26.80	3.41	23.39	6.77
3	0.023	29.64	5.57	24.07	11.90
4	0.023	25.62	5.30	20.32	14.06
5	0.0	1.12	2.01	0	4.90
6	0.0	2.08	4.13	0	10.12

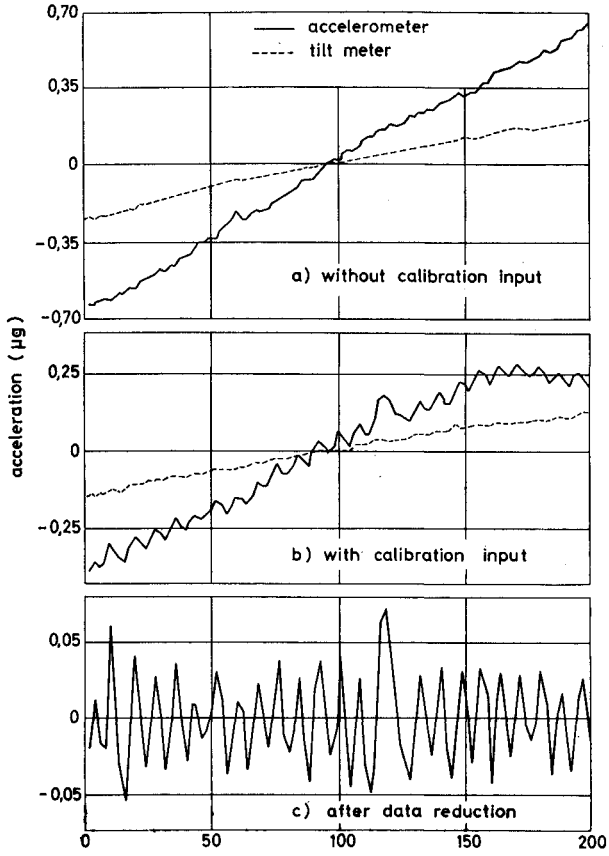

Fig. 3 Accelerometer and tilt meter data.

in the acceptance test of the MESA in the low-g range are: null stability = 0.163×10^{-6} g (4-hr period) and scale factor stability = 0.0175% (±0.1% 4 hr). The mounting of the MESA is a clamp type around the case to get a small distance between the MESA and the lead surface.

A tilt meter made by Ideal Aerosmith was set on the same test pad to measure tilts of the foundation. The surfaces

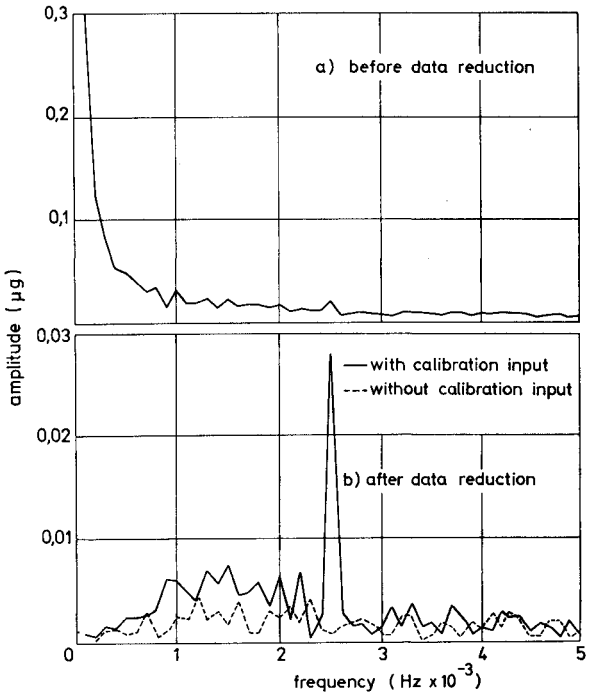

Fig. 4 Fourier analysis of the accelerometer data.

of two interconnected mercury pools 1 m apart serve together with two rigidly mounted plates as two capacitors. Any tilting will change the capacities, which can be expressed in tilt angles. The tilt meter was used in the high-sensitive range. The output of the null meter was calibrated so that a tilt of 0.0067 arcsec produces a voltage of 0.1 v. This voltage was fed into an integrating digital voltmeter. The accelerometer data and the tilt meter data were automatically punched on a paper tape for computer use. The attracting mass, 100 lead cubes of 10.2-cm lengths and 100 lead cubes 5.1-cm lengths, was assembled in the optimized shape. The free spaces in the basket were filled with the same size of wooden cubes.

The time for every measurement was 100 sec. This large measuring time was necessary to get a minimum number of impulses required for statistical data handling. During the measurement, the mass remained in position. At the end of one measurement, the mass was raised or lowered to the next position. The time between the measurements was always 20 sec. In every series at least 100 measurements corresponding to 25 cycles of a sine wave were performed.

The experiment had to show the response of the accelerometer to this small input acceleration. The constant acceleration (or bias) input to the accelerometer, perhaps caused by tilt, was about 17 μg. The setup was very sensitive to temperature changes; therefore, the temperature was controlled in case II (Fig. 2) and was constant to less than 0.1°C.

A tilt change of the accelerometer input axis in the Earth's gravity field of about 0.015 arcsec would create an acceleration input of 0.07 μg. The uncontrolled movement of people in the laboratory stepping on the test pad caused disturbances much larger than 0.1 μg; therefore, almost every experiment was made after working hours when the test room was locked. But even then the tilting of the test pad was observed with the tilt meter during the experiments.

Results and Discussion

The experiment had to show how to measure the small acceleration caused by mass attraction, and how to define the scale factor of the accelerometer for low-acceleration. Because the acceleration input was a relative change, the constant part of the data was removed from the accelerometer data and the tilt meter data. The accelerometer data A_I and the tilt meter B_I have zero mean value. These data are used for the computer analysis.

The random noise was much higher during work time than after work time. The standard deviation from an adjusted curve for the run during work time is twice as much as for the run taken after work time.

The accelerometer and tilt meter data of an experiment are shown in Fig. 3. The response of the accelerometer and the tilt meter to the mass attraction is overlapped by stochastic and other periodic acceleration. But already in the raw data, the movement of the mass is clear (Fig. 3b). The time scale includes the necessary 20 sec for moving the mass. The tilt meter data were multiplied by a scale factor to get radians which correspond to acceleration in g for small angles. The dimensions for the accelerometer data were originally impulses per second. But to give a better impression in all the graphs, the scale factor of the accelerometer data sheet is used to express the data in μg. For every experiment the first position of the lead mass was the middle position followed by the upper position.

The tilt meter data in Fig. 3b show a very small modulation with the frequency of the mass movement. However, it is much less than the corresponding response of the accelerometer. The amplitude of the tilt meter modulation is 0.3×10^{-8} rad for the frequency which corresponds to the movement of the attracting mass. If the accelerometer data were the result of some tilting caused by the mass movement,

the amplitude of the tilt meter output would have to be as high as 3.0×10^{-8} rad for that frequency. The small modulation of the tilt meter data is caused by the mass attraction and is computed in the Appendix. The tilt meter is considered as a supporting device and the analysis is shown only for the accelerometer data.

The accelerometer data are digital, and the analysis is made with a digital computer. A statistical analysis (autocorrelation function and power spectral density) was used together with a Fourier analysis to compute the response of the accelerometer to the small mass attraction input.[5] But just the Fourier analysis is shown in this paper.

The acceleration input is a sine wave with an amplitude of $a_o = 0.023\ \mu g$ and a frequency of 0.0025 Hz. This input frequency corresponds for 100 measurements to a harmonic number of $K = 25$. The enforced response evaluated for a sine wave with a frequency of 0.0025 Hz is the Fourier coefficient. For a sample of 100 data the Fourier coefficient C_{25} is

$$C_{25} = 0.02 \sum_{I=1}^{100} A_I \sin \pi I/2 \qquad (4)$$

The accelerometer data A_I in Fig. 3b show the shape of a saw tooth with the frequency of 0.00025 Hz. Therefore, the Fourier analysis of the data without a data reduction has large amplitudes with low frequencies (Fig. 4a). The Fourier coefficient C_{25} is not just the response to the input sine wave because a certain part of the 25th harmonic is produced by the sawtoothed shape of the over-all data. Therefore, a data reduction was used for the calculation of the scale factor.

The mean value of the data A_I between $I - 3$ and $I + 3$ were subtracted from every A_I. The summation for the mean value was made over 7 points with a weight factor of 1.0 and the two edge points with a weight factor of 0.5. The accelerometer data A_I after this data reduction are shown in Fig. 3c. These data after reduction were used for a Fourier analysis to calculate the accelerometer response to the variated mass attraction input.

The Fourier analysis C_K gives the amplitude as function of the frequency. In Fig. 4b, the amplitudes of two Fourier analyses are shown. The one amplitude distribution is from an experiment without a mass movement. The amplitude at 0.0025 Hz is almost the same as the mean value of the amplitudes at the frequencies from 0.0020 to 0.0030 Hz. The other curve in Fig. 4b is the amplitude distribution of a run with a mass attraction input at a frequency of 0.0025 Hz. The Fourier coefficient C_{25} is 27.80×10^{-2} pps with a frequency of 0.0025 Hz. The mean value, of the amplitudes of the harmonics from $K = 21$ to 24 and $K = 26$ to 29 is as low as 2.17×10^{-2} pps. The amplitude at $K = 25$ is supposed to be a summation of the response to the sine wave input and of some additional random noise. Because 'the bandwidth is limited, the subtraction of the mean random noise level from the amplitude at $K = 25$ is justified. Therefore, the response of the accelerometer to the sine wave input at 0.0025 Hz frequency is 25.63×10^{-2} pps. This value is very close to the computed one with the scale factor for higher acceleration, 23×10^{-2} pps.

For the error calculation, the 20 higher and 20 lower harmonics of the Fourier analysis are subtracted. This does not change the amplitude of the 25th harmonics. After this filtering, the standard deviation from the ideal response sine wave with amplitude C_{25} is calculated. This standard deviation is shown in Table 2 for the different experiments. Run number 1 which was made after work time shows a very low noise level. Runs 2 and 3 were made under almost the same condition, except that the noise level was higher because of the air conditioning equipment. Run number 4 was made during working hours; the data could not be used for scale factor calculations.

The mean value of the response to the mass attraction input is $(24 \pm 2) \times 10^{-2}$ pps for the first three experiments in Table 2. This gives a scale factor of $(1.04 \pm 0.09) \times 10^7$ pps/g for the input amplitude of 0.023 μg. This result is very close to the scale factor of the data sheet in the higher acceleration with 1.02×10^7 pps/g.

The size of the error for the scale factor could be reduced by an improved setup incorporating better noise isolation, and automatic and larger movement of the attracting lead mass. For larger movement of the mass, the amplitude of the input sine wave could be twice as high, and the calibration would be more accurate. The experimental setup was more or less improvised. The aim of the experiments was to prove that the calibration with a mass attraction in the low-g range of 10^{-8} is possible with good confidence and repeatability. The application of these experiments to the calibration of an accelerometer in a satellite for the measurement of the gravity-gradient anomalies of the moon is proposed.

Calibration in Orbit

The suspension force and the range of the MESA is adjustable to the maximum acceleration of the environment. The maximum acceleration in the laboratory is at least 1 g. The maximum acceleration in a satellite could be set to 1 μg after the large acceleration during the boosting phase of the rocket. The center of the satellite is almost under zero-g conditions. The accelerometer can be switched to a very high-sensitive range.

The MESA used for the experiments in the laboratory had just two ranges, but there are instruments with three ranges available for application in space research. A range from 10^{-6} to 10^{-12} should be possible to obtain with a modified MESA in orbit. The scale factor of the MESA would be about 10^6 pps/μg for this very low range. This low threshold produces an acceptable time constant of the system for the proposed measurement of the gravity-gradient anomalies of the moon.

The range of the accelerometer can be adjusted to the accelerations to be measured in orbit, but the accelerometer has to be tested and calibrated in this environment. There are many different unknown acceleration inputs to the accelerometer in a satellite; these are, gravity-gradient acceleration of the orbited planet, mass attraction by the satellite, low-thrust impulses, etc. The mass attraction scheme with a well known but variable acceleration seems to be the best available calibration method for the accelerometer.

A reasonable size of the mass for the calibration of an accelerometer in a satellite might be 1 kg, which sets the upper limit of the acceleration to about 10^{-9} g for a distance of 5.1 cm between the surface of the lead sphere and the proof mass (Table 1). The distance of the lead body remains constant. The angle between the input axis and the mass attraction force is changed to obtain a variable acceleration input with a well-known frequency. The 1 kg lead mass turns around the accelerometer continuously with a very small angular velocity. The input acceleration is a cosine function of the angle between the input axis and the line from the center of the proof mass to the center of the calibrating mass. For easy data handling, the rotation axis of the calibrating mass should go through the center of the accelerometer proof mass. The accelerometer remains in a fixed position to the satellite. If there are no other time variable inputs, the response of the accelerometer is a cosine function with an additional constant caused by the mass attraction of the satellite. With a small computation, the scale factor, nonlinearity, and constant bias of the accelerometer can be calculated. The movement of the mass around the accelerometer can be a continuous one or in steps to facilitate digital analysis. The calibration does not interfere with the experiment and can continue through the whole measurement.

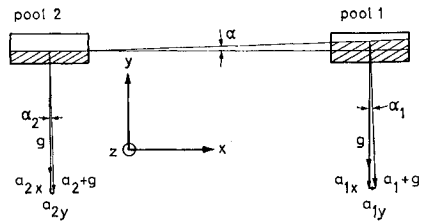

Fig. 5 Mass attraction of the mercury in the tilt meter. (Appendix)

The movement of the calibration mass causes a motion of the center of zero gravity of the satellite and would change the acceleration input by the gravity gradient of the orbited planet with the calibration frequency. Therefore a second smaller mass in a larger distance at the other side of the accelerometer has to rotate around the proof mass of the accelerometer to avoid the movement of the center of zero gravity in the satellite. If the second mass is one tenth of the calibrating mass the distance has to be ten times (about 1 m) the distance of calibrating mass (about 0.1 m) to the rotation axis. The center of zero gravity remains so in a fixed position of the satellite and the accelerometer can be calibrated during the measurement of the gravity gradient of the orbited planet.

The calibrating lead body rotates around the proof mass with an angular velocity of about $3\ 10^{-3}$ rad/sec. At the beginning a disturbance torque of less than 10 dyn cm is produced by the calibrating mass. The attitude control system of the satellite will eliminate this small torque. There are many other disturbances for the calibration of an accelerometer in orbit, but the data filtering with the calibration frequency will eliminate all disturbances with other frequencies.

Summary

The calibration of an accelerometer in the laboratory by the mass attraction method may be of interest in the future, when the low accelerometer thresholds are required. In orbit, the mass attraction scheme is the only presently known practical calibration scheme for accelerations below 10^{-9} g.

Appendix: Mass Attraction of the Tilt Meter (Fig. 5)

The level in the mercury pools of the tilt meter changed with the positions of the attracting mass. Because the distances between the mercury pools and the attracting lead mass are large, the effect is very small. The mercury surface of the tiltmeter pool is always vertical to the acceleration vector consisting of the Earth gravity g and the mass attraction a of the lead assembly. a has a horizontal a_x and a vertical component a_y. The tangent to the surface in pool number 1 has an angle α_1 to the horizontal plane and the tangent to the surface in pool number 2 has an angle α_2. a_{1x} is the horizontal component of a at the position of pool 1

$$tg\alpha_1 = a_{1x}/(g + a_{1y}), \quad tg\alpha_2 = a_{2x}/(g + a_{2y})$$

When α_1, α_2, a_{2y} are very small,

$$\alpha_1 = a_{1x}/g, \quad \alpha_2 = a_{2x}/g$$

A good approximation of the imaginary equipotential surface is a sphere. The line connecting the two pools is the secant line of the circle which is the intersection curve of the sphere with the xy plane. The angle α between the secant line and the x axis is due geometrical correlation

$$\alpha = (\alpha_1 + \alpha_2) \text{ rad}$$

This angle α is the output value of the tilt meter. α was computed for the three positions of the attracting mass

position up	$\alpha_u = 0.680 \times 10^{-8}$ rad
position middle	$\alpha_m = 0.595 \times 10^{-8}$ rad
position down	$\alpha_d = 0.496 \times 10^{-8}$ rad

These values agree to that computed according to the potential theory, too. The movement of the mass causes a tilting of the mercury surface. The input tilting is almost a sine wave with the amplitude of $\alpha_A = (0.1 \pm 0.07) \times 10^{-8}$ rad. The data analysis of the tilt meter data B_I shows an amplitude at the frequency of the mass motion of

$$C_{25} = (0.3 \pm 0.2)10^{-8} \text{ rad}$$

This value has a large standard deviation and is in the same magnitude as the computed amplitude for mass attraction. Therefore, no tilting of the test pad connected with the movement of the attracting mass was large enough to influence the calibration of the MESA in the laboratory.

References

[1] Ganssle, E. R., "Gravity Gradiometry Mission Feasibility Study," CR-24.3, Dec. 1967, NASA.

[2] Plourde, H. S. and Nelson, R. H., "Low Level Accelerometer Test Methods," E-578, June 1965, Dynamic Research Corp., Stoneham, Mass.

[3] McMillan, W. D., *The Theory of the Potential*, Dover, New York, 1958.

[4] Meldrum, M. A., Harrison, E. J., and Milburn, Z., "Development of a Miniature Electrostatic Accelerometer (MESA) for Low g Applications," CR-54137, April 1965, NASA.

[5] Bendat, S. and Piersol, A. G., *Measurement and Analysis of Random Data*, Wiley, New York, Feb. 1967.